Received: 2 September 2022 | Revised: 7 January 2023 | Accepted: 10 January 2023

DOI: 10.1002/mma.9064

SPECIAL ISSUE PAPER

WILEY

Spatial modeling of crime dynamics: Patch and reaction–diffusion compartmental systems

Julia Calatayud[1] | **Marc Jornet**[2] | **Jorge Mateu**[1]

[1]Departament de Matemàtiques, Universitat Jaume I, Castellón, 12071, Spain

[2]Departament de Matemàtiques, Universitat de València, Burjassot, 46100, Spain

Correspondence
Julia Calatayud, Departament de Matemàtiques, Universitat Jaume I, 12071 Castellón, Spain.
Email: calatayj@uji.es

Communicated by: C. Pinto

Funding information
Julia Calatayud has been supported by the postdoctoral contract POSDOC/2021/02 from Universitat Jaume I, Spain (Acció 3.2 del Pla de Promoció de la Investigació de la Universitat Jaume I per a l'any 2021). Jorge Mateu has been supported by the grant PID2019-107392RB-I00 from Spanish Ministry of Science and the grant AICO/2019/198 from Generalitat Valenciana.

We study the dynamics of abstract models for crime evolution. The population is divided into three compartments, taking into account the participation in crime and incarceration. Individuals transit between the three segments, assuming that having more contact with criminally active people increases one's risk of learning and acquiring the same traits; essentially, crime is regarded as a social epidemic. In the literature, there are several models of this type, based on spatial homogeneity and ordinary differential equations. However, these ideas have not been extended to account for spatial variability. Here, we achieve this target with discrete and continuous forms of space: patch and reaction–diffusion compartmental systems, respectively. We build the models and focus on the effect of the basic reproduction number on the long-term dynamics of crime (persistence or disappearance). Several theoretical results are presented, which are supported by numerical simulations.

KEYWORDS

basic reproduction number, crime dynamics, patch compartmental model, reaction–diffusion compartmental model, social epidemic

MSC CLASSIFICATION

34C60, 35B40, 91D25

1 | INTRODUCTION

Compartmental models for infectious disease dynamics divide the population into groups according to the disease state. People may progress between compartments. At the simplest level of modeling, the population is spatially distributed over the geographical region in a homogeneous way; essentially, one considers "spatially averaged" dynamics. This regime is formulated by means of ordinary differential equations (ODEs), which only consider temporal variability. The compartments interact through the coupling of the equations. Some references on these types of models are Hethcote,[1] Brauer,[2] Ma and Li,[3] Acedo et al,[4] and Van Hoek et al.[5]

Of course, for social behaviors related to opinions, attitudes, decisions, and habits, there is no virus transmission. However, peers may serve as a strong stimulus for imitation, especially for behaviors that are socially accepted, cool or profitable.[6,7] Words such as "stimulus," "imitation," "influence," "identification," "pressure," and "persuasion" may be reminiscent of terms used in epidemiology, namely, "contagion," "infection," and "spread." Thus, compartmental

models with nonlinear state dependencies may be of use for the modeling of social behaviors. In the mathematical literature from the last two decades, there are several papers dealing with these ideas, in the contexts of drugs, alcohol, telecommunications, tobacco, excess weight, and so forth.[8–13] We also consider relevant the review papers.[14,15]

In the context of crime modeling,[16] which is the main concern of this paper, the different segments of the population are related to participation in crime and incarceration. People may transit between different behaviors and states. Following the underlying idea of social epidemic, having more contact with criminally active people increases the risk of participating in crime.[17,18] This social transmission point of view for the spread of delinquency has been quite recently adopted in several mathematical papers, with compartmental systems of ODEs.[19–24]

These references about social behavior do not include spatial effects. However, individual attitudes and their transmission obviously depend on habitual location (city, neighborhood, area, and scattering) and travels.[25] Extending ODE-based compartmental models to heterogeneous space may be done by including the ODEs as the reaction terms in a reaction–diffusion partial differential equation (PDE) system, or by treating space as a collection of discrete patches (cities and communities) among which populations may disperse. In the PDE case, diffusion is based on net fluxes of people, conservations, and Fick's law. Movement may be seen as well as the spatial random spread of a two-dimensional Brownian motion, where the "particle" is the person. Under diffusion, low-populated areas tend to receive people from high-populated zones. In the discrete case, the patches yield a larger coupled system of ODEs, with subindices labeling the patch. The dynamics of each patch are coupled to that of other patches by travel. These models are called metapopulation models. Some references, in the context of epidemiological and ecological modeling, are Lloyd and May,[26] van den Driessche,[27] Wu,[28] Schiesser,[29] Kevrekidis et al,[30] and Zhang et al.[31] For crime dynamics with spatial variability, there are several reaction–diffusion PDE models proposed in the literature,[32–39] albeit these do not fall into the category of compartmental equations with interactions. Essentially, space locations are characterized by a risk of criminal activity, taking into account feasibility, attractiveness, opportunities, and knowledge of offenders about target, vulnerability, victims, area, and so forth. The main objective of these contributions is the study of the dynamics of crime hotspots. The power of these theories is the deeper understanding of crime patterns; however, fitting the models to actual crime data is not straightforward.

In the present paper, we focus on the qualitative aspects of mathematical criminology, rather than quantitative aspects with data. But we study the dynamics of crime differently to the cited references, namely, with patch-based coupled ODEs and reaction-diffusion coupled PDEs with a compartmental structure, where interactions between susceptible persons and offenders are present through nonlinear terms and a coefficient capturing the force of influence. To our knowledge, the social transmission viewpoint for the spread of crime has not been treated before with spatial structure via patches or PDEs. A key concept employed here when studying crime dynamics will be the basic reproduction number, that is, the number of influences of a single offender in the society.[40,41] This number is a threshold, which will be used to find out when criminality becomes extinct or endemic in the long run.

The paper is structured as follows. In Section 2, a compartmental system of three ODEs is proposed for the temporal modeling of crime, assuming spatial homogeneity in the region. The flows of people into and out compartments are presented. The basic reproduction number and its relation with the long-term dynamics are exposed. Section 3 completes the previous model by considering spatial effects. We start with a subdivision of the region by interconnected patches, which gives rise to a larger system of ODEs. In Section 4, a different view of spatial heterogeneity is given, by adding diffusion to the ODEs model (reaction part). In both sections, the value of the basic reproduction number and the ensuing dynamics are investigated. Section 5 is devoted to numerical experiments, to illustrate the qualitative behavior of solutions. Finally, the results of the paper and limitations of the approach are commented in Section 6.

2 | HOMOGENEOUS COMPARTMENTAL MODEL

In this section, we present a homogeneous compartmental model for crime evolution along time, composed of ODEs. This is a first step, prior to studying the effect of spatial variations in the following sections. The formulation is similar to that of the first model proposed in McMillon et al,[19] although the interaction term and some flows change slightly and vital dynamics are not considered there.

At each time t, we consider the population divided into the following:

- Susceptible persons, that is, those who are not related to criminal activities (but could be in the future).
- Offenders who are not in prison. This situation may occur when the person has not yet been caught by the police, the offender is waiting for trial, or has been found guilty and is serving sentence but not with penalty of deprivation of liberty.
- Offenders in prison.

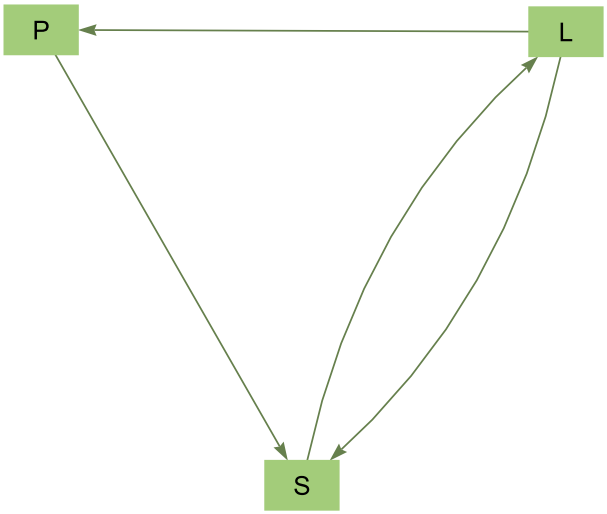

FIGURE 1 Transition diagram of the model, where S, L, and P denote non-offenders, offenders out of prison, and offenders in prison, respectively. [Colour figure can be viewed at wileyonlinelibrary.com]

These define compartments, and individuals flow into and out compartments by assuming the following facts:

- An individual who is not immersed in criminal activities may become an offender by social contact. For example, the person is convinced or pressured, imitates an attitude, and so forth. This follows the principle stating that having more contact with criminally active people increases one's risk of learning and acquiring the same traits. See the references from Section 1.
- An offender who has not been imprisoned may return to the non-offender class. For example, such person has not been caught by the police and decides to desist, has been declared innocent after a trial, or has been condemned but not with deprivation of liberty and the punishment ends.
- An offender, still in liberty, gets imprisoned. This happens after detention, trial, and final judgment.
- A convicted person returns to the non-offender state after completing the term of imprisonment imposed.

These four points are summarized in a transition diagram, in Figure 1.

The model must capture these transitions through averaged coefficients. Let $S(t)$, $L(t)$, and $P(t)$ be the number of non-offenders, offenders out of prison, and offenders in prison, respectively, at time $t \geq 0$. These quantities are related as follows:

$$\begin{cases} \frac{\mathrm{d}S}{\mathrm{d}t} = \Lambda - \beta SL + a_1 L + rP - \mu S, \\ \frac{\mathrm{d}L}{\mathrm{d}t} = \beta SL - a_1 L - a_2 L - \mu L, \\ \frac{\mathrm{d}P}{\mathrm{d}t} = a_2 L - rP - \mu P. \end{cases} \tag{2.1}$$

This is a system of three coupled ODEs, with the following parameters:

- $\Lambda > 0$: Number of births, or new crime-free individuals, per unit time.
- $\mu > 0$: Death rate.
- $\beta > 0$: An offender's force of influence.
- $a_1 > 0$: Rate at which individuals transit from offender into susceptible.
- $a_2 > 0$: Rate at which offenders are incarcerated.
- $r > 0$: Rate at which imprisonment term is completed.

The inverse of μ, a_1, a_2, and r are the average times of transition. Parameter β comes with a nonlinear term, because it is related to interactions. The rest of the parameters come with linear terms, since they depend on single individuals. Notice that the model differs from the classical SIRS formulation due to parameter a_1, since there are transitions from L to S with no imprisonment involved. But, similarly to the SIRS model, there is a recursive flow, because individuals may be incarcerated again after prison release.

A nice interpretation of the parameters is the following. Let $C(t)$ be the number of individuals at instant t in a certain compartment, and let $\mathcal{T}$ be the positive random variable that describes the time of an individual in this compartment.

Given a time lag $h > 0$, it holds $C(t+h) = C(t) - \Pr[\mathcal{T} < t+h | \mathcal{T} \geq t]C(t)$, because $\Pr[\mathcal{T} < t+h|\mathcal{T} \geq t]$ is the proportion of people leaving in the temporal range $[t, t+h)$. By dividing by h and by making h tend to 0, one obtains $\frac{\mathrm{d}C}{\mathrm{d}t} = -\gamma(t)C$, where $\gamma(t)$ is the hazard function of $\mathcal{T}$.[42, p. 13] Thus, in a compartmental model, constant parameter values γ arise when the leaving time is exponentially distributed, with rate given by the parameter. By the maximum entropy principle,[43–45] the exponential distribution is known to be a suitable assignment for positive quantities with a single, averaged estimate (a deterministic estimate of γ^{-1}, for example). We obtain the model $\frac{\mathrm{d}C}{\mathrm{d}t} = -\gamma C$, that is, $C(t+\mathrm{d}t) = C(t) - \gamma \cdot \mathrm{d}t \cdot C(t)$; this means that, for short time spans, a constant proportion of criminals leaves criminality. The parameter γ, being time independent, acts as an averaged exit-time coefficient for a simplification of reality. On the other hand, an interaction term, for example, $\frac{\mathrm{d}S}{\mathrm{d}t} = -\beta SL$, appears when the exit time is described by the hazard function $\gamma(t) = \beta L(t)$; the instantaneous risk of leaving susceptibility depends on the number of offenders, with a force represented by β. Crime dynamics is a complex process, but this high-level perspective on it permits having a crime-free equilibrium to analytically derive a low-crime/high-crime threshold.

The system (2.1) is well posed with three initial conditions: $S(0) = S_0$, $L(0) = L_0$, and $P(0) = P_0$. The total population, $N(t) = S(t) + L(t) + P(t)$, with initial value $N(0) = N_0$, evolves as

$$\frac{\mathrm{d}N}{\mathrm{d}t} = \Lambda - \mu N \;\Rightarrow\; N(t) = \left(N_0 - \frac{\Lambda}{\mu}\right)\mathrm{e}^{-\mu t} + \frac{\Lambda}{\mu}. \tag{2.2}$$

Notice that $N(\infty) = N_\infty = \Lambda/\mu$ (ratio of new susceptible individuals per unit time and death rate), and if $N_0 = N_\infty$, then $N(t)$ is constant and equal to that ratio. Essentially, N_∞ is an equilibrium point for the total population, with the property of being a global attractor.

The system (2.1) preserves positivity when S_0, L_0 and P_0 are greater than 0. Indeed, from the second equation,

$$\frac{\mathrm{d}L}{\mathrm{d}t} = (\beta S - a_1 - a_2 - \mu)L \;\Rightarrow\; L(t) = L_0 \mathrm{e}^{\int_0^t (\beta S(\tau) - a_1 - a_2 - \mu)\mathrm{d}\tau} > 0. \tag{2.3}$$

For the other two compartments, if we assume that S or P may take negative values, then we can pick the first instant of time $t_1 > 0$ at which any of them vanishes. If $P(t_1) = 0$, then

$$\frac{\mathrm{d}P}{\mathrm{d}t}(t_1) = a_2 L(t_1) > 0,$$

which is a contradiction. If $S(t_1) = 0$, then

$$\frac{\mathrm{d}S}{\mathrm{d}t}(t_1) = \Lambda + a_1 L(t_1) + rP(t_1) > 0,$$

which is again a contradiction. Thus, $S(t) > 0$ and $P(t) > 0$ for all $t \geq 0$.

The basic reproduction number $\mathcal{R}_0$ is a concept from epidemiology, defined as the average number of secondary cases produced by one infected individual introduced into a population of susceptible individuals. For social behaviors for which influence plays a key role, one may use $\mathcal{R}_0$ as well. For example, in criminology, $\mathcal{R}_0$ is the mean number of secondary offenders produced by one offender introduced into a population of susceptible individuals. As will be seen, the value of $\mathcal{R}_0$ is essential to control the future of criminal activity.

For model (2.1) in particular, the next-generation matrix method is employed[40,41] to obtain the unknown value of $\mathcal{R}_0$. In the notation used there, conditions[40, (A1)–(A5), p. 161] hold, with

$$\mathcal{F}_1 = \beta SL,\;\; \mathcal{V}_1 = (a_1 + a_2 + \mu)L,$$
$$\mathcal{F}_2 = 0,\;\; \mathcal{V}_2 = -a_2 L + (r + \mu)P.$$

The terms $\mathcal{F}_1$ and $\mathcal{F}_2$ are the rates of appearance of new offenders in compartments L and P, respectively. For L, new offenders arise from interactions. For P, the rate is 0 because people in L are already related to criminal activity. The terms $\mathcal{V}_1$ and $\mathcal{V}_2$ are the rates of other transitions. Given the crime-free equilibrium

$$\mathrm{CFE} = (N_\infty, 0, 0)$$

and the matrices

$$F = \begin{pmatrix} \frac{d\mathcal{F}_1}{dL}(N_\infty,0,0) & \frac{d\mathcal{F}_1}{dP}(N_\infty,0,0) \\ \frac{d\mathcal{F}_2}{dL}(N_\infty,0,0) & \frac{d\mathcal{F}_2}{dP}(N_\infty,0,0) \end{pmatrix} = \begin{pmatrix} \beta N_\infty & 0 \\ 0 & 0 \end{pmatrix},$$
$$V = \begin{pmatrix} \frac{d\mathcal{V}_1}{dL}(N_\infty,0,0) & \frac{d\mathcal{V}_1}{dP}(N_\infty,0,0) \\ \frac{d\mathcal{V}_2}{dL}(N_\infty,0,0) & \frac{d\mathcal{V}_2}{dP}(N_\infty,0,0) \end{pmatrix} = \begin{pmatrix} a_1+a_2+\mu & 0 \\ -a_2 & r+\mu \end{pmatrix},$$

the next-generation matrix is FV^{-1}, and

$$\mathcal{R}_0 = \rho(FV^{-1}) = \frac{\beta N_\infty}{a_1+a_2+\mu}, \tag{2.4}$$

where ρ is the spectral radius. Note that the inverse of the denominator, $1/(a_1+a_2+\mu)$, is the mean time in compartment L. During that time, an offender convinces βN_∞ individuals per unit time, in a society where all citizens are susceptible. For the derivation of $\mathcal{R}_0$, the mathematical model is essential; its value cannot be discerned from descriptive statistics of data.

From the qualitative point of view, the importance of $\mathcal{R}_0$ relies on the following fact[40, Theorem 1]: The CFE is locally asymptotically stable if $\mathcal{R}_0 < 1$, but unstable if $\mathcal{R}_0 > 1$. (For the basics on dynamical systems, the reader is referred to.[46]) Intuitively, when $\mathcal{R}_0 < 1$, each offender convinces less than one person on average, so criminality disappears in the future; when $\mathcal{R}_0 > 1$, by contrast, more than one person is influenced per offender and there are outbreaks that make criminality endemic at the end.

For our model (2.1), the result from Van den Driessche and Watmough[40, Theorem 1] may be extended as follows. If $\mathcal{R}_0 < 1$, then the CFE is globally asymptotically stable (i.e., stable and a global attractor), not only locally. This is a specific, novel result for the model proposed.

Theorem 2.1. *Consider the homogeneous model (2.1), with $\mathcal{R}_0$ given by (2.4). If $\mathcal{R}_0 < 1$, then the CFE is globally asymptotically stable.*

Proof. In this proof, arrows indicate limits as $t \to \infty$. Since $S(t) \le N(t) \to N_\infty$, one has

$$\frac{\beta S(t)}{a_1+a_2+\mu} \le \frac{\beta N(t)}{a_1+a_2+\mu} \to \mathcal{R}_0 < 1,$$

so $\beta S(t) - a_1 - a_2 - \mu < -\epsilon < 0$ for $t \ge T$, for certain $T > 0$ and $\epsilon > 0$. In consequence, from (2.3), $L(t) \to 0$. On the other hand, from the third equation in (2.1),

$$P(t) = e^{-(r+\mu)t}\left[P_0 + \int_0^t a_2 L(s) e^{(r+\mu)s} ds\right].$$

Given any $\delta > 0$, there is a $T_1 > 0$ such that $L(t) < \delta$ for $t > T_1$. Then,

$$P(t) \le e^{-(r+\mu)t}\left[P_0 + a_2\|L\|_\infty \int_0^{T_1} e^{(r+\mu)s} ds + a_2\delta \int_{T_1}^t e^{(r+\mu)s} ds\right] \to \frac{a_2}{r+\mu}\delta, \quad \limsup_{t\to\infty} P(t) \le \frac{a_2}{r+\mu}\delta.$$

As δ is arbitrary, one concludes that $P(t) \to 0$ as well. Finally, $S(t) = N(t) - L(t) - P(t) \to N_\infty$. Therefore, $(S(t), L(t), P(t)) \to$ CFE, independently of the initial conditions (S_0, L_0, P_0), as wanted. □

In summary, when $\mathcal{R}_0 < 1$, then the CFE is globally asymptotically stable, whereas when $\mathcal{R}_0 > 1$, then the CFE is unstable.

In fact, it can be proved that when $\mathcal{R}_0 > 1$, there is a crime-endemic equilibrium that is locally asymptotically stable. This analysis will be left to Section 4, devoted to a reaction–diffusion PDE model, since the ODE case (2.1) will be retrieved for zero diffusion coefficients.

3 | PATCH COMPARTMENTAL MODEL

We now consider a certain spatial region divided into patches (communities). These patches are labeled as $i = 1, \dots, n$. These are not isolated; it is assumed that offenders from patch $j \neq i$ may contact individuals from patch i and transmit their attitude. We use the approach from Lloyd and May[26] and van den Driessche.[27] We define the coupled ODE model

$$\begin{cases} \frac{\mathrm{d}S_i}{\mathrm{d}t} = \Lambda - \left(\sum_{j=1}^{n} \beta_{ij} L_j\right) S_i + a_1 L_i + rP_i - \mu S_i, \\ \frac{\mathrm{d}L_i}{\mathrm{d}t} = \left(\sum_{j=1}^{n} \beta_{ij} L_j\right) S_i - a_1 L_i - a_2 L_i - \mu L_i, \\ \frac{\mathrm{d}P_i}{\mathrm{d}t} = a_2 L_i - rP_i - \mu P_i, \end{cases} \tag{3.1}$$

for $i = 1, \dots, n$. The (positive) parameters are interpreted within each patch as in the single-patch case (2.1), although β_{ij} is now the offender's force of influence from patch j to patch i. There is no explicit movement of individuals in this formulation; instant travels (compared to the unit of time of t) that spread criminality are assumed. The total population, $N_i(t)$, of each patch i satisfies (2.2); in particular, $N_i(\infty) = \Lambda/\mu$ (ratio of new susceptible individuals per unit time on patch i and death rate). Then $N(\infty) = \sum_{i=1}^{n} N_i(\infty) = \frac{\Lambda}{\mu} n$ is the asymptotic population in the whole region (ratio of new susceptible individuals per unit time on the union of the patches and death rate). Finally, when $n = 1$, the three-dimensional ODE system (2.1) is retrieved.

Next, the goal is to compute the basic reproduction number $\mathcal{R}_0$, to discern whether CFE is locally asymptotically stable or unstable from $\mathcal{R}_0 < 1$ or $\mathcal{R}_0 > 1$, respectively. Here, CFE is a $3n$-dimensional vector, where the component corresponding to any S_i is Λ/μ and the rest (those of L_i and P_i) are 0. The next-generation matrix method[40,41] is applicable, as in the previous section, since we still have an ODE system despite the spatial structure. The value of $\mathcal{R}_0$ as a threshold[40, Theorem 1] is applicable too.

In the notation used in literature[40,41] adapted to our situation, we consider the rates

$$\mathcal{F}_i^L = \left(\sum_{j=1}^{n} \beta_{ij} L_j\right) S_i, \ \mathcal{V}_i^L = (a_1 + a_2 + \mu) L_i,$$
$$\mathcal{F}_i^P = 0, \ \mathcal{V}_i^P = -a_2 L_i + (r + \mu) P_i.$$

The terms $\mathcal{F}_i^L$ and $\mathcal{F}_i^P$ are the rates of appearance of new offenders in compartments L_i and P_i, respectively. For L_i, new offenders arise from interactions between S_i and any L_j. For P_i, the rate is 0 because people in L_i are already related to criminal activity. The terms $\mathcal{V}_i^L$ and $\mathcal{V}_i^P$ are the rates of other transitions. Let

$$F = \begin{pmatrix} \frac{\partial \mathcal{F}^L}{\partial L}(\mathrm{CFE}) & \frac{\partial \mathcal{F}^L}{\partial P}(\mathrm{CFE}) \\ \frac{\partial \mathcal{F}^P}{\partial L}(\mathrm{CFE}) & \frac{\partial \mathcal{F}^P}{\partial P}(\mathrm{CFE}) \end{pmatrix}, \ V = \begin{pmatrix} \frac{\partial \mathcal{V}^L}{\partial L}(\mathrm{CFE}) & \frac{\partial \mathcal{V}^L}{\partial P}(\mathrm{CFE}) \\ \frac{\partial \mathcal{V}^P}{\partial L}(\mathrm{CFE}) & \frac{\partial \mathcal{V}^P}{\partial P}(\mathrm{CFE}) \end{pmatrix},$$

be defined by four $n \times n$ blocks, where $\mathcal{F}^L$, $\mathcal{F}^P$, $\mathcal{V}^L$, $\mathcal{V}^P$, L, and P are interpreted as n-dimensional vectors. Then, simple calculations show

$$F = \begin{pmatrix} \frac{\Lambda}{\mu} B & 0_n \\ 0_n & 0_n \end{pmatrix}, \ V = \begin{pmatrix} (a_1 + a_2 + \mu) I_n & 0 \\ -a_2 I_n & (r + \mu) I_n \end{pmatrix},$$

where $B = (\beta_{ij})_{1 \leq i,j \leq n}$, 0_n is the $n \times n$ zero matrix, and I_n is the $n \times n$ identity matrix. Given

$$V^{-1} = \begin{pmatrix} \frac{1}{a_1 + a_2 + \mu} I_n & 0_n \\ \frac{a_2}{(a_1 + a_2) r} I_n & \frac{1}{r + \mu} I_n \end{pmatrix},$$

the next-generation matrix becomes

$$FV^{-1} = \begin{pmatrix} \frac{\Lambda}{\mu(a_1 + a_2 + \mu)} B & 0_n \\ 0_n & 0_n \end{pmatrix}.$$

Therefore, the basic reproduction number takes the form

$$\mathcal{R}_0 = \frac{\Lambda}{\mu(a_1 + a_2 + \mu)}\rho(B),$$

where ρ is the spectral radius. This expression for $\mathcal{R}_0$ clearly extends that of a single patch from the previous section. In terms of $N(\infty) = \frac{\Lambda}{\mu}n$, $\mathcal{R}_0$ may be rewritten as

$$\mathcal{R}_0 = \frac{N(\infty)\rho(B)}{a_1 + a_2 + \mu}\frac{1}{n}. \tag{3.2}$$

Note that the factor $1/n$ appears in (3.2). This makes sense, as there are more patches and the larger the dispersion is, there are more difficulties to transmit crime because the probability of a contact is lower.

According to Van den Driessche and Watmough,[40, Theorem 1] the CFE is locally asymptotically stable if $\mathcal{R}_0 < 1$, but unstable if $\mathcal{R}_0 > 1$. As in the previous section, we may go beyond[40, Theorem 1] and prove that, when $\mathcal{R}_0 < 1$, the CFE is globally asymptotically stable, not only locally.

Theorem 3.1. *Consider the metapopulation model (3.1), with $\mathcal{R}_0$ given by (3.2). If $\mathcal{R}_0 < 1$, then the CFE is globally asymptotically stable.*

Proof. In this proof, arrows indicate limits as $t \to \infty$. Since $S_i(t) \le N_i(t) \to \Lambda/\mu$, we have

$$\frac{S_i(t)\rho(B)}{a_1 + a_2 + \mu} \le \frac{N_i(t)\rho(B)}{a_1 + a_2 + \mu} \to \mathcal{R}_0 < 1.$$

In consequence, there are $\epsilon > 0$ and $T > 0$ such that

$$\frac{S_i(t)\rho(B)}{a_1 + a_2 + \mu} < 1 - \epsilon, \ \forall t \ge T.$$

Therefore,

$$S_i(t) < \frac{a_1 + a_2 + \mu}{\rho(B)}(1 - \epsilon), \ \forall t \ge T.$$

In consequence, from the second equation in (3.1), for $t \ge T$,

$$\frac{\mathrm{d}L_i}{\mathrm{d}t} < \frac{a_1 + a_2 + \mu}{\rho(B)}\left[(1 - \epsilon)\sum_{j=1}^{n}\beta_{ij}L_j - \rho(B)L_i\right] = (\tilde{B}L)_i,$$

where

$$\tilde{B} = \frac{a_1 + a_2 + \mu}{\rho(B)}[(1 - \epsilon)B - \rho(B)I_n]$$

and $L = (L_1, \ldots, L_n)^\top$ (here $\top$ denotes the transpose). Let $\tilde{L} = (\tilde{L}_1, \ldots, \tilde{L}_n)^\top$ such that

$$\frac{\mathrm{d}\tilde{L}}{\mathrm{d}t} = \tilde{B}\tilde{L}, \ \tilde{L}(T) = L(T).$$

Then the estimates $L_i(t) < \tilde{L}_i(t)$ hold, for $t \ge T$ and $i = 1, \ldots, n$, see previous studies[47,48] (each term $(\tilde{B}L)_i$ is non-decreasing with respect to the arguments L_j, for all $j \ne i$). To prove that $L_i(t) \to 0$, it suffices to see that $\tilde{L}_i(t) \to 0$; that is, the eigenvalues of $\tilde{B}$ have negative real part. The eigenvalues $\tilde{\lambda}$ of $\tilde{B}$ are of the form

$$\tilde{\lambda} = \frac{a_1 + a_2 + \mu}{\rho(B)}[(1 - \epsilon)\lambda - \rho(B)],$$

where λ is an eigenvalue of B. Hence,

$$\begin{aligned}\Re(\tilde{\lambda}) &= \frac{a_1+a_2+\mu}{\rho(B)}[(1-\epsilon)\Re(\lambda)-\rho(B)] \leq \frac{a_1+a_2+\mu}{\rho(B)}[(1-\epsilon)\rho(B)-\rho(B)] \\ &= -(a_1+a_2+\mu)\epsilon < 0,\end{aligned}$$

as wanted.

From the third equation in (3.1), which only depends on i explicitly, one deduces that $P_i(t) \to 0$ as in the proof of Theorem 2.1. Finally, $S_i(t) = N_i(t) - L_i(t) - P_i(t) \to \Lambda/\mu$. Therefore, $(S(t), L(t), P(t)) \to$ CFE, independently of the initial conditions. □

4 | REACTION–DIFFUSION COMPARTMENTAL MODEL

We now develop the final model. Consider a certain open and bounded spatial region $\Omega \subseteq \mathbb{R}^2$, with smooth boundary $\partial\Omega$ and area $|\Omega|$. This region may be a city, a community, a country, etc., represented in a map, with smoothed borders. The citizens of Ω are divided into three compartments: susceptible to crime, offenders who are not in prison, and offenders in prison. Let $S \equiv S(x, y, t)$ be the number of susceptible persons per unit area at (x, y, t). Let $L \equiv L(x, y, t)$ be the number of out-of-prison offenders per unit area at (x, y, t). Finally, let $P \equiv P(x, y, t)$ be the number, per unit area, of imprisoned individuals at time t that were caught at (x, y) (after release, they will return to S at (x, y), as if they had been quarantined during an infection). In contrast to ODEs, the three compartments are now population densities, rather than absolute numbers (masses).

Taking into account the ODE model (2.1) as a reaction and the diffusive spread of individuals, the model proposed is the following one

$$\begin{cases} \frac{\partial S}{\partial t} = D_S\Delta S + \Lambda - \beta SL + rP + a_1L - \mu S, \\ \frac{\partial L}{\partial t} = D_L\Delta L + \beta SL - a_1L - a_2L - \mu L, \\ \frac{\partial P}{\partial t} = a_2L - rP - \mu P. \end{cases} \tag{4.1}$$

Here, $\Delta = \frac{\partial^2}{\partial x^2} + \frac{\partial^2}{\partial y^2}$ is the Laplacian operator, $D_S > 0$ and $D_L > 0$ are the diffusion constants that incorporate spatial variability, $\Lambda > 0$ is the constant number of births or new crime-free individuals per unit time and unit area, $\mu > 0$ is the death rate, $\beta > 0$ is the force of influence of criminal activity through interactions, $r > 0$ is the rate of release from prison, $a_1 > 0$ is the rate from out-of-prison offender to susceptibility, and $a_2 > 0$ is the rate of the transition from offender to imprisoned. (Note that here Λ is interpreted per unit area, as a constant density, in contrast to the ODE case; both "recruitment" parameters are thus different, by the factor $|\Omega|$.) Notice that $D_P = 0$, because people in prison do not diffuse. The flow parameters r, a_1 and a_2 take the same value as in the ODE case (2.1), because they involve processes occurring at the level of a single individual, that is, "locally," and hence, we do not expect them to change at the spatial level in the transition from the ODE to the PDE model. On the contrary, we do not expect this to be the case for the transmission rate β, since it depends on the interaction between individuals and their scattering.[30]

To determine the densities in space for all future times $t > 0$, initial distributions are needed:

$$S(x, y, 0) = S_0(x, y),\ L(x, y, 0) = L_0(x, y),\ P(x, y, 0) = P_0(x, y),\ \forall (x, y) \in \Omega \cup \partial\Omega.$$

For a bounded space, we need to specify boundary states. We consider that there is no significant immigration or emigration, through homogeneous Neumann boundary conditions:

$$\frac{\partial S}{\partial n}(x, y, t) = 0,\ \frac{\partial L}{\partial n}(x, y, t) = 0,\ \frac{\partial P}{\partial n}(x, y, t) = 0,\ \forall (x, y) \in \partial\Omega,\ \ \forall t > 0, \tag{4.2}$$

where $n(x, y)$ is the outward unit normal vector on $\partial\Omega$.

As in the ODE case (2.1), it is of interest to investigate the positivity of solutions and the evolution of the total population $N(t)$ in the region.

Theorem 4.1. *Given the PDE system (4.1) with homogeneous Neumann boundary conditions (4.2), the densities S, L and P are positive for every time, if the initial densities S_0, L_0 and P_0 are. On the other hand, the total population*

$$N(t) = \int_\Omega S(x,y,t)\,\mathrm{d}x\mathrm{d}y + \int_\Omega L(x,y,t)\,\mathrm{d}x\mathrm{d}y + \int_\Omega P(x,y,t)\,\mathrm{d}x\mathrm{d}y$$

satisfies

$$\frac{\mathrm{d}N}{\mathrm{d}t} = \Lambda|\Omega| - \mu N \;\Rightarrow\; N(t) = \left(N_0 - \frac{\Lambda}{\mu}|\Omega|\right)\mathrm{e}^{-\mu t} + \frac{\Lambda}{\mu}|\Omega|.$$

In particular,

$$N(\infty) = \frac{\Lambda|\Omega|}{\mu} = \frac{\textit{new susceptible individuals per unit time on } \Omega}{\textit{death rate}},$$

as in the ODE case (2.1).

Proof. For the positivity preservation, we need to check that the reaction part is quasi-positive.[49,50] If

$$\begin{aligned} f_1(s,l,p) &= \Lambda - \beta sl + rp + a_1 l - \mu s,\\ f_2(s,l,p) &= \beta sl - a_1 l - a_2 l - \mu l,\\ f_3(s,l,p) &= a_2 l - rp - \mu p, \end{aligned}$$

and $s,l,p \geq 0$, then $f_1(0,l,p) = \Lambda + rp + a_1 l \geq 0$, $f_2(s,0,p) = 0 \geq 0$ and $f_3(s,l,0) = a_2 l \geq 0$, and we are done.

For the population conservation, we integrate the PDEs from (4.1):

$$\begin{aligned} \frac{\partial}{\partial t}\int_\Omega S(x,y,t)\,\mathrm{d}x\mathrm{d}y &= D_S\int_\Omega \Delta S(x,y,t)\,\mathrm{d}x\mathrm{d}y + \Lambda|\Omega| - \beta\int_\Omega S(x,y,t)L(x,y,t)\,\mathrm{d}x\mathrm{d}y\\ &\quad + r\int_\Omega P(x,y,t)\,\mathrm{d}x\mathrm{d}y + a_1\int_\Omega L(x,y,t)\,\mathrm{d}x\mathrm{d}y - \mu\int_\Omega S(x,y,t)\,\mathrm{d}x\mathrm{d}y,\\ \frac{\partial}{\partial t}\int_\Omega L(x,y,t)\,\mathrm{d}x\mathrm{d}y &= D_L\int_\Omega \Delta L(x,y,t)\,\mathrm{d}x\mathrm{d}y + \beta\int_\Omega S(x,y,t)L(x,y,t)\,\mathrm{d}x\mathrm{d}y\\ &\quad - (a_1+a_2)\int_\Omega L(x,y,t)\,\mathrm{d}x\mathrm{d}y - \mu\int_\Omega L(x,y,t)\,\mathrm{d}x\mathrm{d}y\\ \frac{\partial}{\partial t}\int_\Omega P(x,y,t)\,\mathrm{d}x\mathrm{d}y &= a_2\int_\Omega L(x,y,t)\,\mathrm{d}x\mathrm{d}y - r\int_\Omega P(x,y,t)\,\mathrm{d}x\mathrm{d}y - \mu\int_\Omega P(x,y,t)\,\mathrm{d}x\mathrm{d}y. \end{aligned}$$

From the Neumann boundary conditions,

$$\int_\Omega \Delta S(x,y,t)\,\mathrm{d}x\mathrm{d}y = \int_\Omega \nabla\cdot\nabla S(x,y,t)\,\mathrm{d}x\mathrm{d}y = \int_{\partial\Omega}\underbrace{\nabla S(x,y,t)\cdot n(x,y)}_{\frac{\partial S}{\partial n}(x,y,t)}\mathrm{d}\mathcal{S}(x,y) = 0,$$

where the divergence theorem[51] has been used. Here, $\nabla = \left(\frac{\partial}{\partial x}, \frac{\partial}{\partial y}\right)$ denotes the gradient operator, the dot is the scalar product, and $\mathrm{d}\mathcal{S}$ is an infinitesimal surface area. For L,

$$\int_\Omega \Delta L(x,y,t)\,\mathrm{d}x\mathrm{d}y = 0$$

analogously holds. By adding the three integral equations, we obtain the desired ODE for N. □

Next, the aim is to investigate the existence of a tipping point for the extinction or the persistence of crime. We take

$$\mathcal{R}_0 = \frac{\Lambda}{\mu}\frac{\beta}{a_1+a_2+\mu} = \frac{\beta N(\infty)}{a_1+a_2+\mu}\frac{1}{|\Omega|}. \tag{4.3}$$

Notice that, compared with the ODE situation (2.1), we consider the same threshold but divided by $|\Omega|$. This makes sense, as the larger the region and the dispersion are, there are more difficulties to transmit crime because the probability of a contact is lower. The same fact occurred with the multi-patch case (3.1).

Theorem 4.2. *Consider the PDE system (4.1) with homogeneous Neumann boundary conditions (4.2). Let $\mathcal{R}_0$ be given by (4.3). If $\mathcal{R}_0 < 1$, then the crime-free equilibrium*

$$CFE = \left(\frac{\Lambda}{\mu}, 0, 0\right)$$

is locally asymptotically stable. On the other hand, if $\mathcal{R}_0 > 1$, then the CFE is unstable and the crime-endemic equilibrium

$$CEE = \left(\frac{a_1 + a_2 + \mu}{\beta}, \frac{(\mu + r)(\mathcal{R}_0 - 1)(a_1 + a_2 + \mu)}{\beta(\mu + a_2 + r)}, \frac{a_2(\mathcal{R}_0 - 1)(a_1 + a_2 + \mu)}{\beta(\mu + a_2 + r)}\right)$$

is locally asymptotically stable.

Proof. Let $E = (S, L, P)^\top$ and let $\bar{E} = (\bar{S}, \bar{L}, \bar{P})^\top$ be a spatially homogeneous equilibrium point (i.e., the reaction part vanishes at it). For the ODE case, the stability of a fixed point is studied through the linearized system. Here, we do the same. The linearized PDE approximates the reaction part, $f = (f_1, f_2, f_3)^\top$, through its Jacobian at the equilibrium point $\bar{E}$:

$$f(e) \approx f(\bar{E}) + J(e - \bar{E}) = J(e - \bar{E}),$$

where $e \in [0, \infty)^3$ and

$$J = Jf(\bar{E}) = \begin{pmatrix} -\beta\bar{L} - \mu & a_1 - \beta\bar{S} & r \\ \beta\bar{L} & -a_1 - a_2 + \beta\bar{S} - \mu & 0 \\ 0 & a_2 & -r - \mu \end{pmatrix}.$$

That is, locally around $\bar{E}$, terms of order $\mathcal{O}((e - \bar{E})^2)$ are disregarded. If $D = \operatorname{diag}(D_S, D_L, 0)$ is the diffusion matrix, then the linearized PDE is

$$\frac{\partial E}{\partial t} = D\Delta E + J(E - \bar{E}), \tag{4.4}$$

with homogeneous Neumann boundary conditions,

$$\frac{\partial E}{\partial n} = 0 \text{ on } \partial\Omega. \tag{4.5}$$

Given the Laplacian PDE problem

$$\begin{cases} -\Delta\varphi = \lambda\varphi \text{ on } \Omega, \\ \frac{\partial\varphi}{\partial n} = 0 \text{ on } \partial\Omega, \end{cases}$$

we consider the set of its eigenvalues, $\{\lambda_i\}_{i=0}^{\infty} \subseteq [0, \infty)$, repeated with multiplicity, with $\lambda_0 = 0$ and $\lambda_i \nearrow \infty$, and the set of associated eigenfunctions $\{\varphi_i\}_{i=0}^{\infty}$ with norm equal to 1 in $L^2(\Omega)$. These eigenfunctions form a complete orthonormal system in $L^2(\Omega)$. That is, any square integrable function on Ω can be expanded as a Fourier series in terms of $\{\varphi_i\}_{i=0}^{\infty}$. See Jost.[52, Theorem 11.5.2]

Given a solution E of (4.4)–(4.5), and an equilibrium point $f(\bar{E}) = 0$, write

$$E(x, y, t) - \bar{E} = \sum_{i=0}^{\infty} v_i(t)\varphi_i(x, y), \tag{4.6}$$

where $v_i(t) = \int_\Omega (E(x, y, t) - \bar{E})\varphi_i(x, y)\mathrm{d}x\mathrm{d}y \in \mathbb{R}^3$ is the Fourier coefficient. By substituting (4.6) into (4.4), we obtain

$$\frac{\mathrm{d}v_i}{\mathrm{d}t} = A_i v_i, \; A_i = J - \lambda_i D.$$

It is well-known that $\lim_{t\to\infty} v_i(t) = 0$ if and only if the eigenvalues of A_i have negative real part; otherwise, 0 is unstable. Thus,

$$p_i(\lambda) = \det(J - \lambda_i D - \lambda I_3) = 0, \tag{4.7}$$

where I_3 is the identity matrix, is the key equation; indeed, if $\Re(\lambda) < 0$ for every root λ and every $i \geq 0$, then $\bar{E}$ is locally asymptotically stable; but if $\Re(\lambda) > 0$ for some root λ and some $i \geq 0$, then $\bar{E}$ is unstable. We will work with $\bar{E} = \text{CFE}$ and $\bar{E} = \text{CEE}$.

When $\bar{E} = \text{CFE}$, Equation (4.7) is

$$p_i(\lambda) = (-\lambda_i D_S - \mu - \lambda)(-a_1 - a_2 - \lambda_i D_L + \beta\Lambda/\mu - \mu - \lambda)(-r - \mu - \lambda) = 0,$$

for $i \geq 0$. The three roots are

$$\lambda = -\lambda_i D_S - \mu < 0, \lambda = -a_1 - a_2 - \lambda_i D_L + \beta\Lambda/\mu - \mu = -\lambda_i D_L + (\mathcal{R}_0 - 1)(a_1 + a_2 + \mu) < 0, \text{ for } s\mathcal{R}_0 < 1,$$

and

$$\lambda = -r - \mu < 0.$$

Thus, when $\mathcal{R}_0 < 1$, the three roots are negative for all $i \geq 0$, so CFE is locally asymptotically stable. If $\mathcal{R}_0 > 1$, then the second root is positive for $i = 0$, therefore CFE is unstable.

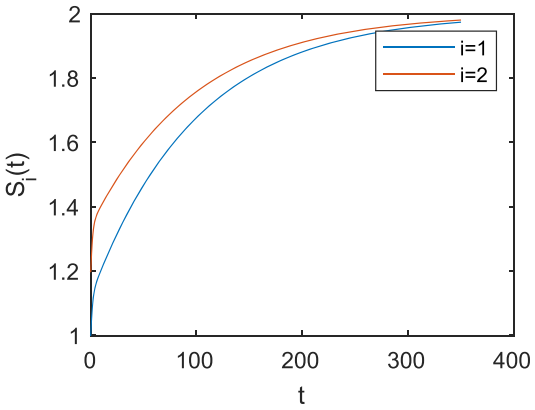

FIGURE 2 Example 5.1. Case $\mathcal{R}_0 < 1$. Evolution of the susceptible compartments $S_i(t)$ with time. [Colour figure can be viewed at wileyonlinelibrary.com]

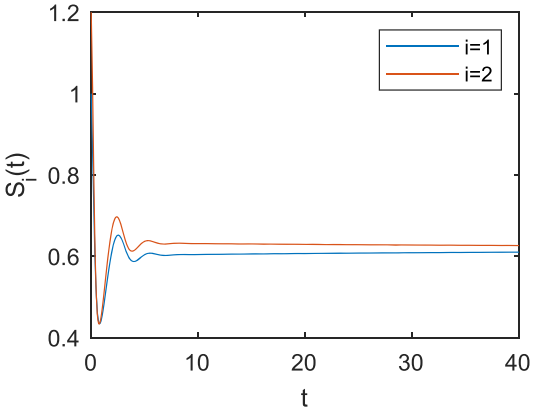

FIGURE 3 Example 5.1. Case $\mathcal{R}_0 > 1$. Evolution of the susceptible compartments $S_i(t)$ with time. [Colour figure can be viewed at wileyonlinelibrary.com]

The analysis of the CEE, which only exists when $\mathcal{R}_0 > 1$, is more cumbersome. After algebraic manipulations in a symbolic software, Equation (4.7) takes the form

$$p_i(\lambda) = -\lambda^3 - b\lambda^2 - c\lambda - d = 0,$$

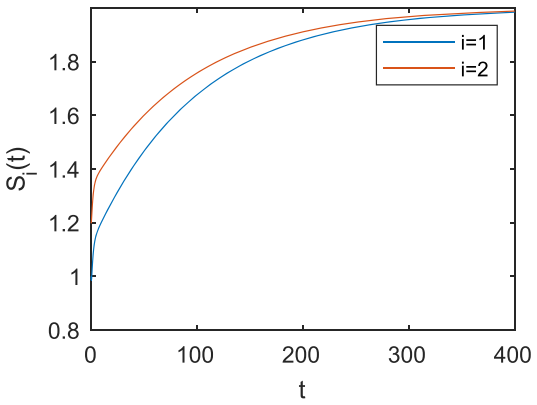

FIGURE 4 Example 5.1. Case $\mathcal{R}_0 = 1$. Evolution of the susceptible compartments $S_i(t)$ with time. [Colour figure can be viewed at wileyonlinelibrary.com]

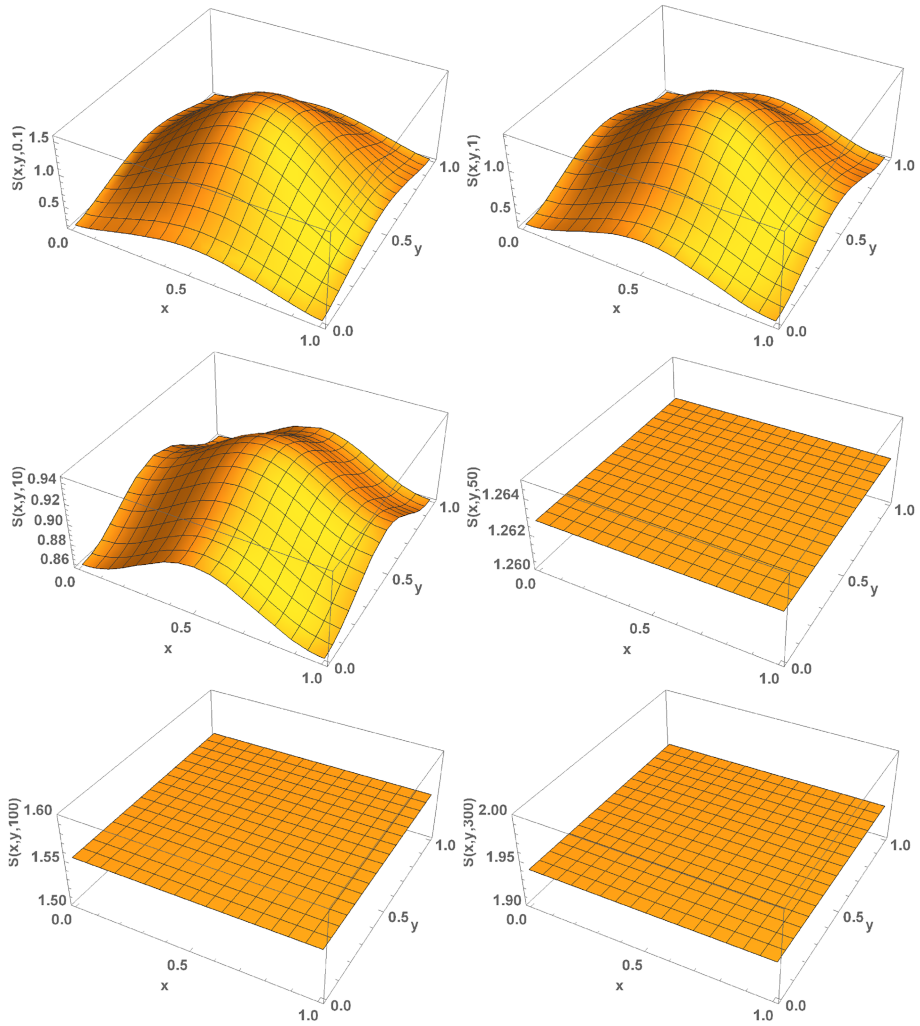

FIGURE 5 Example 5.2. Case $\mathcal{R}_0 < 1$. Evolution of the susceptible compartment $S(x, y, t)$ with time. [Colour figure can be viewed at wileyonlinelibrary.com]

where

$$
\begin{aligned}
b = \frac{1}{a_2+\mu+r}\Big[&a_2\mu + (\mathcal{R}_0-1)a_1(\mu+r) + 2\mu r + \mathcal{R}_0\mu^2 + \mu^2 \\
&+ r^2 + (D_L+D_S)(a_2+\mu+r)\lambda_i + \mathcal{R}_0 a_2\mu + \mathcal{R}_0 a_2 r + \mathcal{R}_0\mu r\Big] > 0,\\
c = \frac{1}{a_2+\mu+r}\Big[&(2\mathcal{R}_0-1)\mu^3 + 2(\mathcal{R}_0-1)a_1\mu^2 + (3\mathcal{R}_0-2)a_2\mu^2 + (\mathcal{R}_0-1)a_2^2\mu \\
&+ (\mathcal{R}_0-1)(a_1+a_2)r^2 + (\mathcal{R}_0-1)a_2^2 r + (3\mathcal{R}_0-1)\mu^2 r + (\mathcal{R}_0-1)a_1a_2(\mu+r) \\
&+ 3(\mathcal{R}_0-1)a_1\mu r + (4\mathcal{R}_0-3)a_2\mu r + (D_L+D_S)\lambda_i(\mu^2+r^2) + \mathcal{R}_0\mu r^2 \\
&+ D_LD_S\lambda_i^2(a_2+\mu+r) + D_L\mathcal{R}_0\lambda_i\mu^2 + (\mathcal{R}_0-1)D_La_1\lambda_i(\mu+r) + (D_L+D_S)a_2\lambda_i\mu \\
&+ D_Sa_2\lambda_i r + 2(D_L+D_S)\lambda_i\mu r + D_L\mathcal{R}_0\lambda_i(a_2\mu + a_2 r + \mu r)\Big] > 0
\end{aligned}
$$

and

$$
\begin{aligned}
d = \frac{1}{a_2+\mu+r}\Big[&(\mathcal{R}_0-1)\left(\mu^4 + a_1\mu^3 + 2a_2\mu^3 + 2\mu^3 r + a_2^2\mu^2 + \mu^2 r^2 + a_1a_2\mu^2 + 2\mu^3 r\right. \\
&+ a_1\mu r^2 + 2a_1\mu^2 r + a_2\mu r^2 + 3a_2\mu^2 r + a_2^2\mu r + a_1a_2\mu r + D_La_1\lambda_i(\mu^2+r^2) + D_La_2\lambda_i r^2 \\
&\left.+ D_La_1\lambda_i\mu r + D_La_2\lambda_i\mu r\right) \\
&+ D_L\mathcal{R}_0\lambda_i\left(\mu^3 + \mu r^2 + 2\mu^2 r + a_2\mu r\right) + D_LD_S\lambda_i^2\left(\mu^2 + r^2 + a_2\mu + a_2 r + a_2\mu^2 + 2\mu r\right)\Big] > 0.
\end{aligned}
$$

Since $b > 0$, $d > 0$ and $bc > d$ (this last condition may be verified in a symbolic software), the Routh-Hurwitz criterion states that the real parts of the roots are negative,[53] independently of $i \geq 0$. Therefore, CEE is locally asymptotically stable, as wanted. □

Remark 4.3. Another common approach for studying the dynamics of PDEs consists in perturbing the solution of the linearized PDE (4.4) as

$$
\begin{aligned}
S(x,y,t) &= \bar{S} + v_1 e^{\lambda t} e^{i(kx+ly)},\\
L(x,y,t) &= \bar{L} + v_2 e^{\lambda t} e^{i(kx+ly)},\\
P(x,y,t) &= \bar{P} + v_3 e^{\lambda t} e^{i(kx+ly)},
\end{aligned}
$$

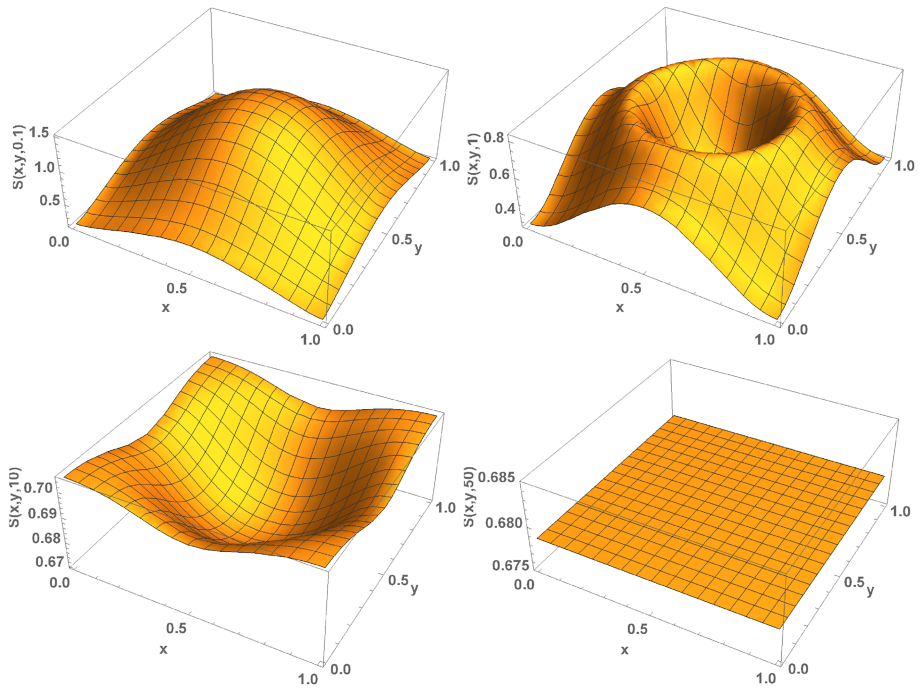

FIGURE 6 Example 5.2. Case $\mathcal{R}_0 > 1$. Evolution of the susceptible compartment $S(x, y, t)$ with time. [Colour figure can be viewed at wileyonlinelibrary.com]

where $\bar{E} = (\bar{S}, \bar{L}, \bar{P})$ is the spatially homogeneous equilibrium point at hand, and i is the imaginary unit. The parameters (k, l) and λ represent the wave vector and the growth rate of the perturbations around $\bar{E}$, respectively. This point $\bar{E}$ is locally asymptotically stable if $\Re(\lambda) < 0$ for any $k, l, v_1, v_2, v_3 \in \mathbb{R}$; otherwise, if $\Re(\lambda) > 0$ for some $k, l, v_1, v_2, v_3 \in \mathbb{R}$, then it is unstable. Equation (4.7) is obtained, but with $\lambda_{k,l} = k^2 + l^2$ instead of λ_i. At the end, the conclusions about $\Re(\lambda)$ and the stability of $\bar{E}$ are the same. With this approach, which works in practice, one is employing the eigenfunctions $e^{i(kx+ly)}$ of $-\Delta$ associated to $\lambda_{k,l}$, but the boundary condition (4.5) is not satisfied.

Remark 4.4. When $\Lambda = \mu = 0$, that is, no vital dynamics are assumed, then the population $N(t)$ is steady along time. Proceeding as we did, eigenvalues with zero real part are obtained in (4.7) for $i = 0$. Then, stability or instability of CFE and CEE cannot be ascertained. This might be a case of Turing instability,[54] and further analysis would be required.

5 | NUMERICAL EXPERIMENTS

In this section, we present numerical simulations to illustrate the theoretical findings. There are three numerical examples. The first example is devoted to the patch model (see Section 3), while the second and third examples deal with the PDE model (see Section 4) on a rectangular and non-rectangular spatial region, respectively. The focus is put on the evolution of the compartments as the time t passes, for fixed input coefficients. For t large, we check that the displayed

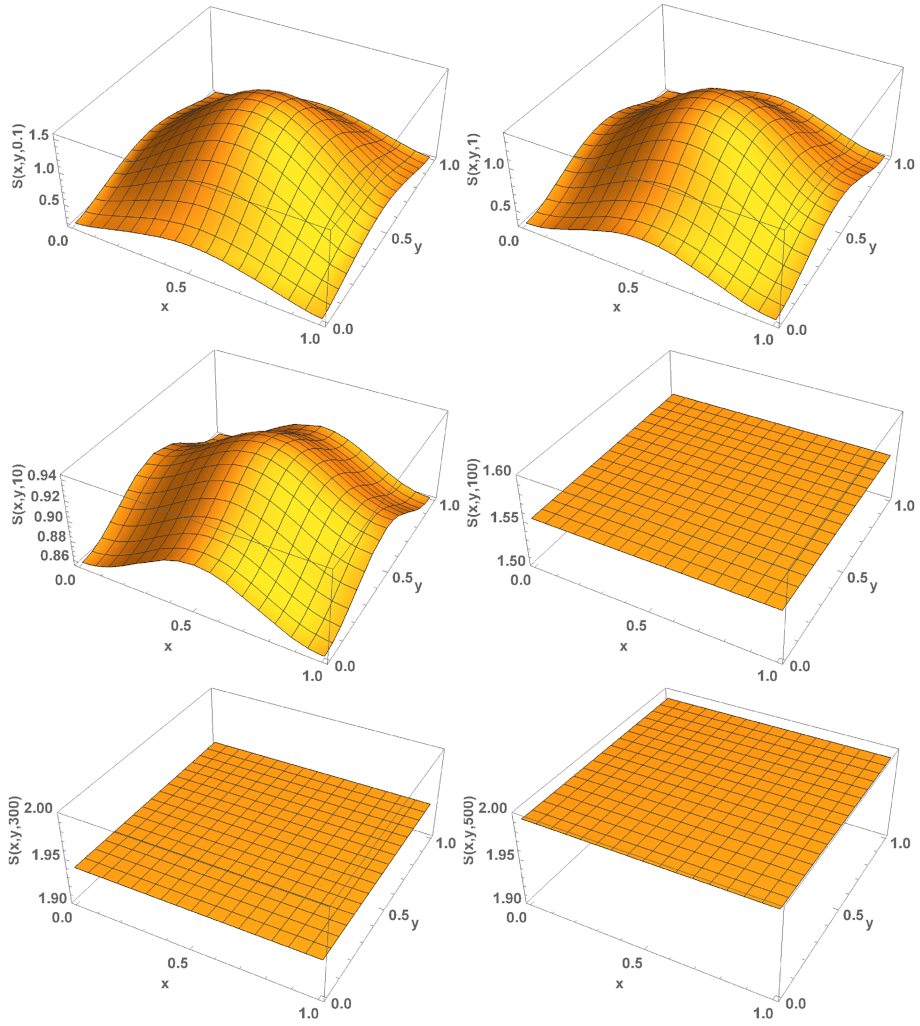

FIGURE 7 Example 5.2. Case $\mathcal{R}_0 = 1$. Evolution of the susceptible compartment $S(x, y, t)$ with time. [Colour figure can be viewed at wileyonlinelibrary.com]

dynamics are in agreement with the value of $\mathcal{R}_0$. In each example, three situations are considered: $\mathcal{R}_0 < 1$, $\mathcal{R}_0 > 1$ and $\mathcal{R}_0 = 1$. We have used the software *Matlab*[55] and *Mathematica*.[56]

Example 5.1. Consider a spatial region with two fragmented areas, labeled as $i = 1$ and $i = 2$. Fix the coefficients of the patch model (3.1), $\Lambda = 0.02$, $\mu = 0.01$, $\beta_{11} = \beta_{22} = 1.2$, $\beta_{12} = \beta_{21} = 1$, $r = 0.6667$, $a_1 = 1.7143$ and $a_2 = 5.2174$, with initial conditions $S_1(0) = 1$, $S_2(0) = 1.2$, $L_1(0) = 0.1$, $L_2(0) = 0.1$, $P_1(0) = 0.02$ and $P_2(0) = 0.04$. These values are considered so as to yield $\mathcal{R}_0 < 1$ and to have interpretable results.

There are two communities, which interact by short-term movements. Citizens transit between the three compartments of their patch. If t is measured in years, the average time in prison is $1/r = 1.5$ years. The average time of the transition $L \to S$ is $1/a_1 = 0.5833$, that is, 7 months. The mean time of the transition $L \to P$ is $1/a_2 = 0.1917$, that is, 2.3 months. The asymptotic populations are $N_i(\infty) = 2$ (this is some sort of scaled problem).

These values of the coefficients yield an $\mathcal{R}_0$ (see (3.2)) less than 1. In Figure 2, we plot the evolution of $S_1(t)$ and $S_2(t)$, by solving the patch model (3.1) with the Runge–Kutta scheme. Both compartments converge to $\Lambda/\mu = 2$, as predicted by the theoretical analysis.

Now consider the same parameter values, but with higher transmission coefficients $\beta_{11} = \beta_{22} = 10.23$. This change gives an $\mathcal{R}_0$ (see (3.2)) greater than 1. In Figure 3, we show that $S_1(t)$ and $S_2(t)$ do not converge to $\Lambda/\mu = 2$ and that there is an endemic equilibrium, which is approached in an oscillatory way.

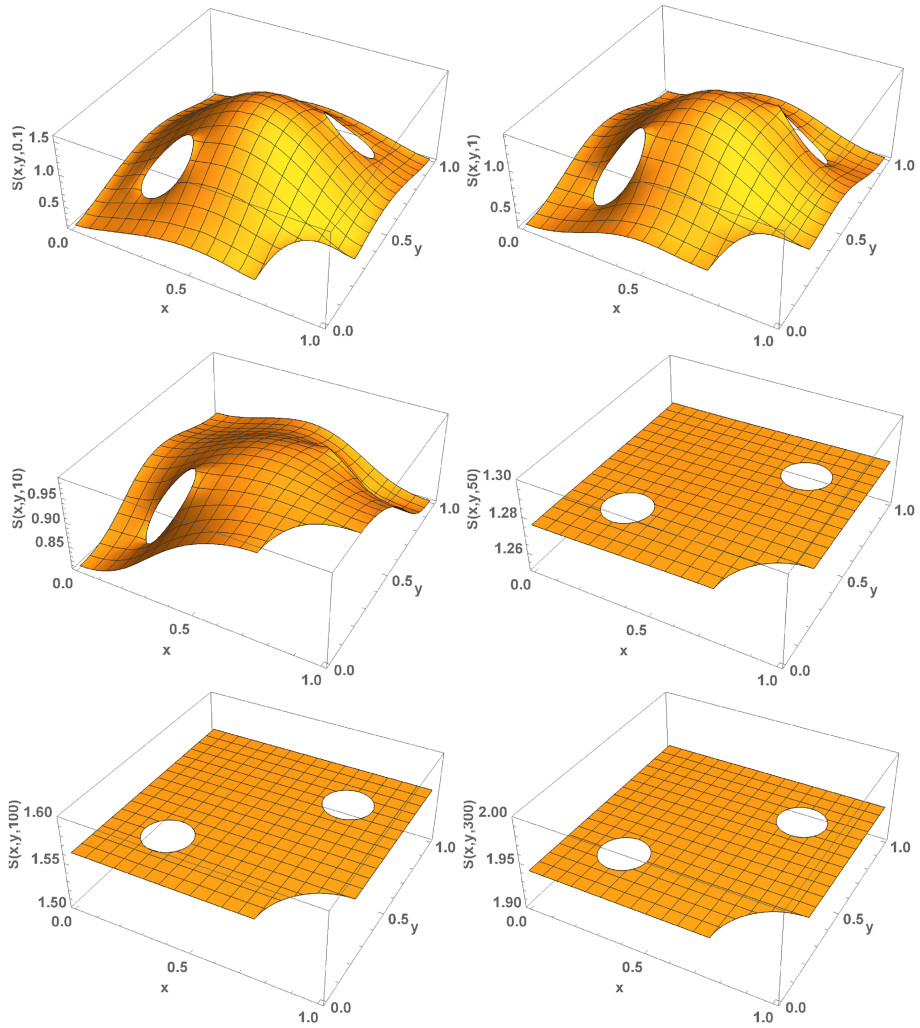

FIGURE 8 Example 5.3. Case $\mathcal{R}_0 < 1$. Evolution of the susceptible compartment $S(x, y, t)$ with time. [Colour figure can be viewed at wileyonlinelibrary.com]

Finally, we modify the transmission coefficients so that $\mathcal{R}_0 = 1$ (see (3.2)). We take $\beta_{11} = \mu(a1 + a2 + \mu)/\Lambda = 3.4708$, $\beta_{12} = 0$, $\beta_{21} = 1$ and $\beta_{22} = 1$. The case $\mathcal{R}_0 = 1$ has not been analyzed theoretically. But, in Figure 4, we see that $S_1(t)$ and $S_2(t)$ converge to the asymptotic population $\Lambda/\mu = 2$. It seems that, for $\mathcal{R}_0 = 1$, the CFE is a global attractor

Example 5.2. Consider the two-dimensional domain $\Omega = (0, 1) \times (0, 1)$. Fix the coefficients of the PDE model (4.1), $D_S = 0.0069$, $D_L = 0.00069$, $\Lambda = 0.02$, $\mu = 0.01$, $\beta = 1.1528$, $r = 0.6667$, $a_1 = 1.7143$ and $a_2 = 5.2174$, with initial conditions $S_0(x, y)$, $L_0(x, y)$ and $P_0(x, y)$ of the form $c\,\mathcal{N}(x, y; \mu, kI_2)$, for $(x, y) \in \Omega$, where $\mathcal{N}$ represents a multivariate Gaussian density, with $c = 0.998$, $c = 0.00163$, and $c = 0.00037$, respectively, $\mu = (0.5, 0.5)^\top$, and $k = 0.1$, $k = 0.01$ and $k = 0.01$, respectively.

This is a test example to support the theoretical results of the paper numerically. People are living in a square and diffuse. Initially, most of the population density is located at the center of the square; the center may be viewed as an important zone of a community, where the majority of the population and delinquents are initially concentrated. As time passes, citizens transit between the three compartments and spread along the region. As in the first example, if t is measured in years, the average time in prison is $1/r = 1.5$ years, the average time of the transition $L \to S$ is $1/a_1 = 0.5833$, that is, 7 months, and the mean time of the transition $L \to P$ is $1/a_2 = 0.1917$, that is, 2.3 months. The asymptotic population is $N(\infty) = 2$ (this is some sort of scaled problem).

For these values of the coefficients, $\mathcal{R}_0$ given by (4.3) is less than 1. The PDE problem may be discretized with a classical finite-difference scheme, taking into account the Neumann boundary conditions. In Figure 5, the different plots show the evolution of $S(x, y, t)$ as time t increases. When t becomes large, $S(x, y, t)$ tends to $\Lambda/\mu = 2$, as predicted by the theoretical results.

Now consider the same parameter values, but the force of influence is augmented to $\beta = 10.23$ in the PDE model (4.1). This makes $\mathcal{R}_0$ (given by (4.3)) greater than 1. In Figure 6, the temporal evolution of $S(x, y, t)$ is illustrated. When t increases, it tends to $(a_1 + a_2 + \mu)/\beta = 0.679$.

Finally, we set $\beta = \mu(a1+a2+\mu)/\Lambda = 3.4708$, so that $\mathcal{R}_0 = 1$ (see (4.3)). This situation was not analyzed theoretically, but we believe that the CFE is an attractor. In Figure 7, we illustrate how $S(x, y, t)$ converges to $\lambda/\mu = 2$ as time increases.

Example 5.3. We proceed as in Example 5.2, but now the spatial domain Ω is defined as follows: consider the square $(0, 1) \times (0, 1)$ but removing the closed disks centered at $(0.25, 0.25)$, $(0.75, 0.75)$ and $(1, 0)$ with radius 0.1,

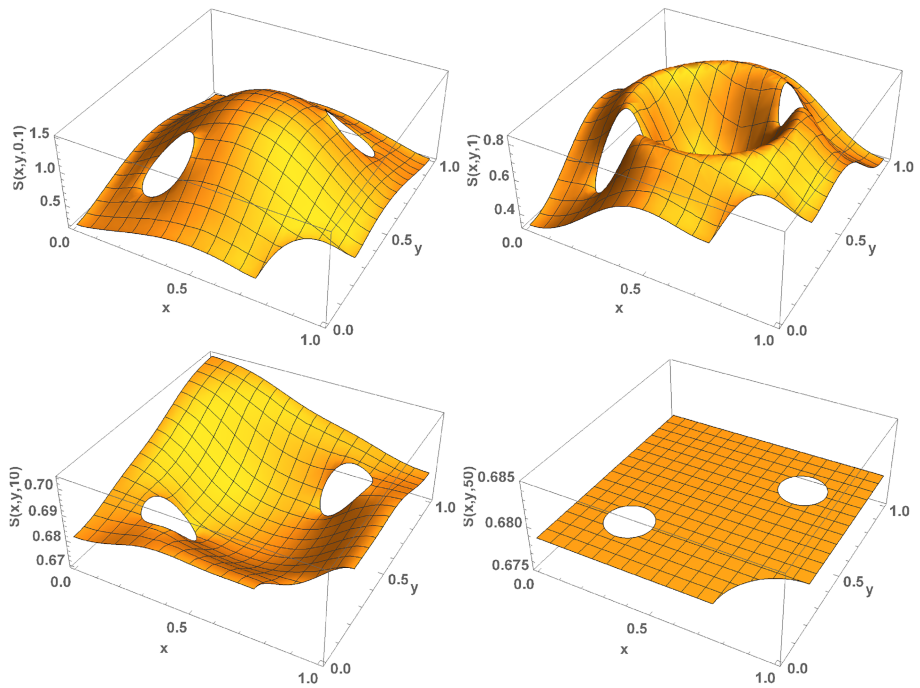

FIGURE 9 Example 5.3. Case $\mathcal{R}_0 > 1$. Evolution of the susceptible compartment $S(x, y, t)$ with time. [Colour figure can be viewed at wileyonlinelibrary.com]

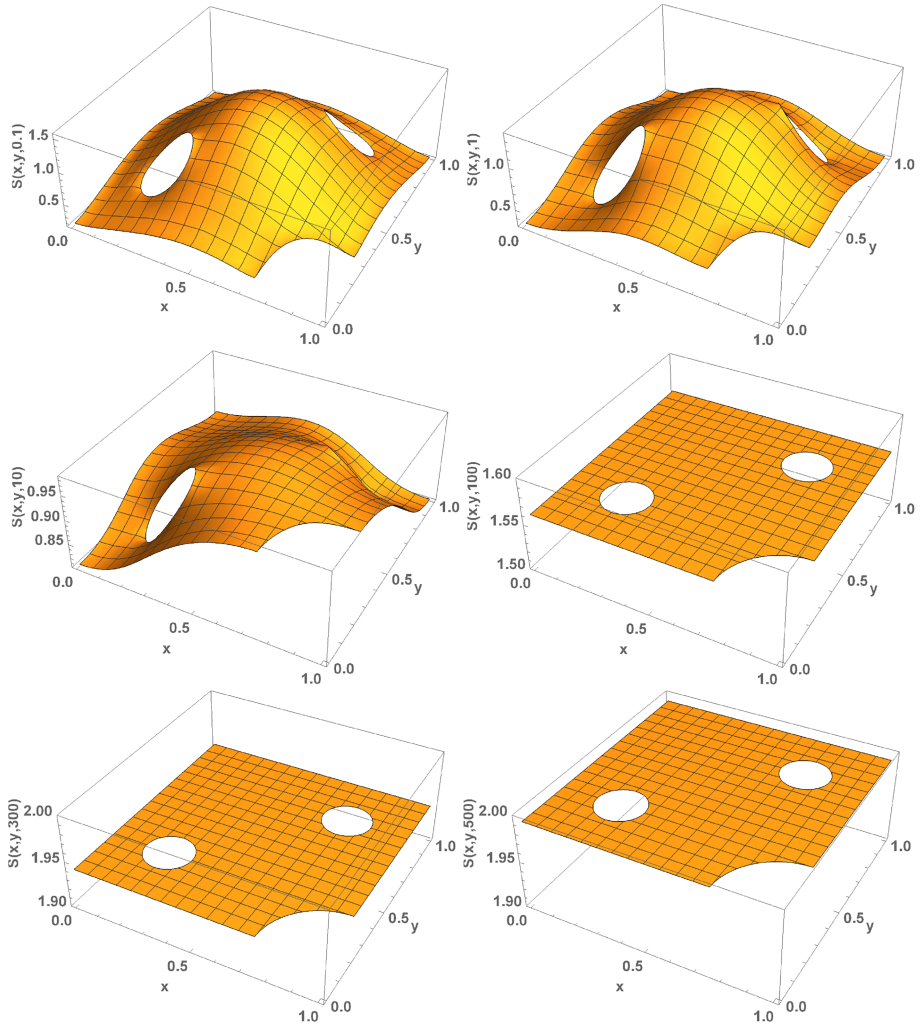

FIGURE 10 Example 5.3. Case $\mathcal{R}_0 = 1$. Evolution of the susceptible compartment $S(x, y, t)$ with time. [Colour figure can be viewed at wileyonlinelibrary.com]

0.1 and 0.25, respectively. To solve the PDE problem (4.1) with homogeneous Neumann boundary conditions, the finite element method has been used (software *Mathematica*, package *"NDSolve'FEM',"* domain specification with *ImplicitRegion*, and PDE resolution with *NDSolveValue* with appropriate initial conditions and automatic boundary condition). Figures 8–10 are analogous to Figures 5–7: They show the evolution of $S(x, y, t)$ as time t increases, for the three cases $\mathcal{R}_0 < 1$, $\mathcal{R}_0 > 1$, and $\mathcal{R}_0 = 1$. The asymptotic dynamics coincide, independently of the spatial domain.

6 | CONCLUSIONS

As reviewed in the Introduction section, there are several contributions on the temporal modeling of crime as a social epidemic, by using compartmental systems of ODEs. Regarding spatial effects in the setting of differential equations, reaction-diffusion PDEs have been proposed for depicting crime hotspots, taking into account attractiveness of locations. However, to our knowledge, compartmental systems of ODEs incorporating a social transmission viewpoint of crime have not been extended to the spatial domain. In the present paper, we achieve this target with discrete and continuous forms of space. The former case gives a metapopulation model, in which space is divided into patches that communicate by short-term movements. The latter case is based on reaction-diffusion compartmental PDEs, which consider that individuals diffuse; the trajectories of a reflecting two-dimensional Brownian motion capture the movement of the persons. We focus on a model with three basic compartments: people susceptible to crime, out-of-prison offenders, and incarcerated persons. The transition from susceptibility into delinquency occurs by social interactions that influence decisions to

participate in crime. The main goal of our investigation is the study of the long-term dynamics of the model, in the three different versions: spatial homogeneity, patch distinction, and diffusive movement. The basic reproduction number, $\mathcal{R}_0$, is a basic tool for the analysis, as it acts as a threshold of stability for the CFE. The main novelties and results of the paper are the following:

- The proposal of new spatial models of crime, based on differential equations, compartments and social interactions.
- The calculation of $\mathcal{R}_0$ for our particular models.
- Spatially homogeneous model: When $\mathcal{R}_0 < 1$, then the CFE is globally asymptotically stable; when $\mathcal{R}_0 > 1$, then the CFE is unstable and the CEE is locally asymptotically stable. This result extends the usual application of $\mathcal{R}_0$ from the literature that gives *local* asymptotic stability of CFE, not *global*, and instability of CFE.
- Patch model: If $\mathcal{R}_0 < 1$, then the CFE is globally asymptotically stable; if $\mathcal{R}_0 > 1$, then the CFE is unstable. Again, this result extends the usual application of $\mathcal{R}_0$ from the literature that gives *local* asymptotic stability of CFE, not *global*.
- Reaction-diffusion PDE: When $\mathcal{R}_0 < 1$, then the CFE is locally asymptotically stable; when $\mathcal{R}_0 > 1$, then the CFE is unstable and the CEE is locally asymptotically stable. This result is new, since the usual application of $\mathcal{R}_0$ from the literature is aimed at ODEs, not PDEs.

The results are proved rigorously and are supported by numerical simulations. There are three numerical examples. The first example is devoted to the patch model, while the second and third examples deal with the PDE model on a rectangular and a non-rectangular spatial region, respectively. Runge–Kutta, finite difference and finite element methods are applied, respectively. In each example, three situations are considered: $\mathcal{R}_0 < 1$, $\mathcal{R}_0 > 1$, and $\mathcal{R}_0 = 1$. From numerical evidence, we believe that the CFE is globally asymptotically stable when $\mathcal{R}_0 \leq 1$ and that the CEE is globally asymptotically stable when $\mathcal{R}_0 > 1$.

This paper has several limitations, which define potential avenues of research:

- From the mathematical viewpoint, some situations regarding the value of $\mathcal{R}_0$ are still open. For example, the case $\mathcal{R}_0 = 1$ is unclear yet. Also, the global stability of the CFE when $\mathcal{R}_0 < 1$ is not proved in the PDE context. The analysis of the global stability of the CEE is also lacking in the three sections.
- We use the fact that social interactions influence decisions to participate in crime. If this is the only manner of becoming active in crime, then there is a CFE (indeed, for a sufficiently small force of influence, crime is eradicated). However, it is recognized that there are individual differences in the propensity toward crime. Individuals may become criminals by own decisions. This type of transition may be included in models and analyze the new equilibria.
- Data are not included. This paper presents basic theoretical models and their qualitative analysis, as a precursor to work with real data. In this context, data fitting is not easy: Patch models suffer from the curse of dimensionality, while reaction–diffusion PDE models on rough spatial domains are complex.

CONFLICT OF INTEREST STATEMENT

The authors declare that there is no conflict of interests regarding the publication of this article.

DATA AVAILABILITY STATEMENT

Data sharing is not applicable as no new data are generated.

ORCID

Julia Calatayud https://orcid.org/0000-0002-9639-1530
Marc Jornet https://orcid.org/0000-0003-0748-3730
Jorge Mateu https://orcid.org/0000-0002-2868-7604

REFERENCES

1. Hethcote HW. The mathematics of infectious diseases. *SIAM Rev*. 2000;42(4):599-653.
2. Brauer F. Compartmental models in epidemiology. In: Brauer F, van den Driessche P, Wu J, eds. *Mathematical Epidemiology*. Berlin, Heidelberg: Springer; 2008:19-79.
3. Ma Z, Li J. *Dynamical Modelling and Analysis of Epidemics*. London: World Scientific; 2009.
4. Acedo L, Díez-Domingo J, Morano JA, Villanueva RJ. Mathematical modelling of respiratory syncytial virus (RSV): vaccination strategies and budget applications. *Epidemiol Infection*. 2010;138(6):853-860.

5. Van Hoek AJ, Melegarob A, Zaghenid E, Edmundsa WJ, Gayb N. Modelling the impact of a combined varicella and zoster vaccination programme on the epidemiology of varicella zoster virus in England. *Vaccine*. 2011;29:2411-2420.
6. Blanchflower DG, Oswald AJ, Landeghem BV. Imitative obesity and relative utility. *J Eur Econ Assoc*. 2009;7:528-538.
7. Harkins SG, Williams KD, Burger J. *The Oxford Handbook of Social Influence*. UK: Oxford University Press; 2017.
8. Song B, Castillo-Garsow M, Ros-Soto KR, Mejran M, Henso L, Castillo-Chávez C. Raves, clubs and ecstasy: the impact of peer pressure. *Math Biosci Eng*. 2006;3(1):249-266.
9. White E, Comiskey C. Heroin epidemics, treatment and ODE modeling. *Math Biosci*. 2017;208(1):312-324.
10. Santonja FJ, Sánchez E, Rubio M, Morera JL. Alcohol consumption in Spain and its economic cost: a mathematical modeling approach. *Math Comput Model*. 2010;52(7–8):999-1003.
11. Cervelló R, Cortés JC, Santonja FJ, Villanueva RJ. The dynamics over the next few years of the Spanish mobile telecommunications market share: a mathematical modelling approach. *Math Comp Model Dyn*. 2014;20(6):557-565.
12. Casabán MC, Cortés JC, Navarro-Quiles A, Romero JV, Roselló MD, Villanueva RJ. A comprehensive probabilistic solution of random SIS-type epidemiological models using the random variable transformation technique. *Commun Nonlinear Sci Numer Simulat*. 2016;32:199-210.
13. Calatayud J, Jornet M. Mathematical modeling of adulthood obesity epidemic in Spain using deterministic, frequentist and Bayesian approaches. *Chaos Soliton Fract*. 2020;140:110179.
14. Sooknanan J, Comissiong DM. When behaviour turns contagious: the use of deterministic epidemiological models in modeling social contagion phenomena. *Int J Dyn Control*. 2017;5(4):1046-1050.
15. Koss L. SIR models: differential equations that support the common good. *CODEE J*. 2019;12(6):61-71.
16. Bertozzi AL, Johnson SD, Ward MJ. Mathematical modelling of crime and security. *Eur J Appl Math*. 2016;27:311-316.
17. Burgess RL, Akers RL. A differential association-reinforcement theory of criminal behavior. *Soc Probl*. 1966;14(2):128-147.
18. Esiri MO. The influence of peer pressure on criminal behaviour. *J Human Social Sci*. 2016;21(1):08-14.
19. McMillon D, Simon CP, Morenoff J. Modeling the underlying dynamics of the spread of crime. *PLoS ONE*. 2014;9(4):e88923.
20. Misra A. Modeling the effect of police deterrence on the prevalence of crime in the society. *Appl Math Comput*. 2014;237:531-545.
21. Abbas S, Tripathi JP, Neha AA. Dynamical analysis of a model of social behavior: criminal vs non-criminal population. *Chaos Soliton Fract*. 2017;98:121-129.
22. González-Parra G, Chen-Charpentier B, Kojouharov HV. Mathematical modeling of crime as a social epidemic. *J Interdiscip Math*. 2018;21(3):623-643.
23. Srivastav AK, Ghosh M, Chandra P. Modeling dynamics of the spread of crime in a society. *Stoch Anal Appl*. 2019;37(6):991-1011.
24. Srivastav AK, Athithan S, Ghosh M. Modeling and analysis of crime prediction and prevention. *Soc Netw Anal Min*. 2020;10(1):1-21.
25. Eck JE, Weisburd D. Crime places in crime theory. *Crime and Place: Crime Prevention Studies*. Criminal Justice Press; 1995:1-33.
26. Lloyd A, May RM. Spatial heterogeneity in epidemic models. *J Theor Biol*. 1996;179:1-11.
27. van den Driessche P. Compartmental models in epidemiology. *Mathematical Epidemiology*. Berlin, Heidelberg: Springer; 2008:179-189.
28. Wu J. Spatial structure: Partial differential equations models. *Mathematical Epidemiology*. Berlin, Heidelberg: Springer; 2008:191-203.
29. Schiesser WE. *Spatiotemporal Modeling of Influenza. Partial Differential Equation Analysis in R Synthesis Lectures on Biomedical Engineering*. USA: Morgan & Claypool Publishers; 2019.
30. Kevrekidis PG, Cuevas-Maraver J, Drossinos Y, Rapti Z, Kevrekidis GA. Reaction-diffusion spatial modeling of COVID-19: Greece and Andalusia as case examples. *Phys Rev E*. 2021;104(2):024412.
31. Zhang B, DeAngelis DL, Ni WM. Carrying capacity of spatially distributed metapopulations. *Trends in Ecol Evol*. 2021;36(2):164-173.
32. Short MB, Brantingham PJ, Bertozzi AL, Tita GE. Dissipation and displacement of hotspots in reaction-diffusion models of crime. *Proc Natl Acad Sci*. 2010;107(9):3961-3965.
33. Rodriguez N, Bertozzi A. Local existence and uniqueness of solutions to a PDE model for criminal behavior. *Math Models Methods Appl Sci*. 2010;20(supp01):1425-1457.
34. Short M, Bertozzi A, Brantingham P. Nonlinear patterns in urban crime: hotspots, bifurcations, and suppression. *SIAM J Appl Dyn Syst*. 2010;9(2):462-483.
35. Manásevich R, Phan QH, Souplet P. Global existence of solutions for a chemotaxis-type system arising in crime modelling. *Eur J Appl Math*. 2013;24:273-296.
36. Berestycki H, Rodriguez N, Ryzhik L. Traveling wave solutions in a reaction-diffusion model for criminal activity. *Multiscale Model Simul*. 2013;11:1097-1126.
37. Kolokolnikov T, Ward MJ, Wei J. The stability of steady-state hot-spot patterns for a reaction-diffusion model of urban crime. *Discret Contin Dyn Syst - B*. 2014;19:1373-1410.
38. Tse WH, Ward MJ. Hotspot formation and dynamics for a continuum model of urban crime. *Eur J Appl Math*. 2015;27:583-624.
39. Gu Y, Wang Q, Yi G. Stationary patterns and their selection mechanism of urban crime models with heterogeneous near-repeat victimization effect. *Eur J Appl Math*. 2017;28(1):141-178.
40. Van den Driessche P, Watmough J. Further notes on the basic reproduction number. *Mathematical Epidemiology*. Berlin, Heidelberg: Springer; 2008:159-178.
41. Van den Driessche P. Reproduction numbers of infectious disease models. *Infectious Disease Model*. 2017;2(3):288-303.
42. Evans M, Hastings N, Peacock B. *Statistical Distributions*. 3rd ed. New York: Wiley; 2000.
43. Dorini FA, Sampaio R. Some results on the random wear coefficient of the Archard model. *J Appl Mech*. 2012;79(5):051008-051014.

44. Muñoz-Cobo JL, Mendizábal R, Miquel A, Berna C, Escrivá A. Use of the principles of maximum entropy and maximum relative entropy for the determination of uncertain parameter distributions in engineering applications. *Entropy*. 2017;19(9):486.
45. BIPM, IEC, IFCC, ILAC, ISO, IUPAC, IUPAP, OIML. Evaluation of Measurement Data - Supplement 1 to the "Guide to the Expression of Uncertainty in Measurement" - Propagation of distributions using a Monte Carlo method. Bureau International des Poids et Mesures JCGM 101; 2008.
46. Teschl G. *Ordinary Differential Equations and Dynamical Systems*, Vol. 140. Providence, USA: Graduate Studies in Mathematics, American Mathematical Society; 2012.
47. Wazewski T. Systèmes de équations et des inégalités différentielles ordinaires aux deuxièmes membres monotones et leurs applications. *Ann Soc Polon Math*. 1950;23:112-166.
48. Hazewinkel M. *Encyclopaedia of Mathematics: Coproduct-Hausdorff-Young Inequalities*, Vol. 2. Dordrecht: Springer; 1995.
49. Smoller J. *Shock Waves and Reaction-Diffusion Equations Berlin*. Germany: Springer; 1983.
50. Pierre M. Global existence in reaction-diffusion systems with control of mass: a survey. *Milan J Math*. 2010;78(2):417-455.
51. Salsa S. *Partial Differential Equations in Action: From Modelling to Theory*. Milan: Springer; 2016.
52. Jost J. *Partial Differential Equations*. 3rd ed. New York: Graduate Texts in Mathematics, Springer; 2013.
53. Ivanescu M. Control. In: Marghitu DB, ed. *Engineer's, Mechanical*. USA: Handbook Academic Press, Academic Press Series in Engineering; 2001:611-714.
54. Gambino G, Lombardo MC, Sammartino M. Turing instability and traveling fronts for a nonlinear reaction-diffusion system with cross-diffusion. *Math Comput Simul*. 2012;82(6):1112-1132.
55. TheMath Works, Inc. *MATLAB Version 2021b*. Massachusetts: Natick; 2021.
56. Wolfram Research, Inc. *Mathematica Version 12.1*. Champaign: IL; 2020.

How to cite this article: Calatayud J, Jornet M, Mateu J. Spatial modeling of crime dynamics: Patch and reaction–diffusion compartmental systems. *Math Meth Appl Sci*. 2023;1-20. doi:10.1002/mma.9064